AD-A181 168 MEASURING AND MODELLING THE TRANSITION LAYER DURING THE 1/1
DISSOLUTION OF GR (U) CORNELL UNIV ITHACA SCHOOL OF
CHEMICAL ENGINEERING P D KRASICKY ET AL 29 MAY 87
UNCLASSIFIED TR-5 N00014-85-K-0474 F/G 7/6 NL

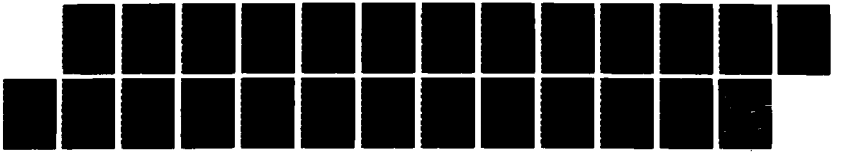

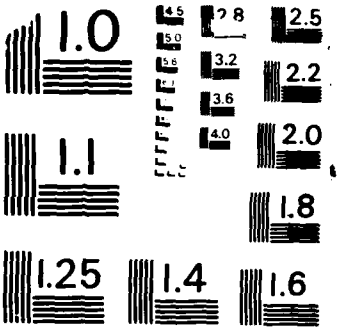

MICROCOPY RESOLUTION TEST CHART

NATIONAL BUREAU OF STANDARDS-1963-A

(12)

OFFICE OF NAVAL RESEARCH

Contract N00014-85-K-0474

Technical Report No. 5

MEASURING AND MODELLING THE TRANSITION LAYER DURING THE DISSOLUTION OF GLASSY POLYMER FILMS

by

P. D. Krasicky, R. J. Groele, and F. Rodriguez

Olin Hall, Cornell University
School of Chemical Engineering
Ithaca, NY 14853

Prepared for presentation at the
National Meeting of the American Institute of Chemical Engineers
Boston, August 24-27, 1987

SECURITY CLASSIFICATION OF THIS PAGE (When Data Entered)

REPORT DOCUMENTATION PAGE

READ INSTRUCTIONS BEFORE COMPLETING FORM

1. REPORT NUMBER: 5	2. GOVT ACCESSION NO.
3. RECIPIENT'S CATALOG NUMBER	
4. TITLE (and Subtitle): Measuring and Modelling the Transition Layer During the Dissolution of Glassy Polymer Films	5. TYPE OF REPORT & PERIOD COVERED: Technical Report
	6. PERFORMING ORG. REPORT NUMBER
7. AUTHOR(s): P. D. Krasicky, R. J. Groele, F. Rodriguez	8. CONTRACT OR GRANT NUMBER(s)
9. PERFORMING ORGANIZATION NAME AND ADDRESS: Cornell University, Ithaca, NY 14853	10. PROGRAM ELEMENT, PROJECT, TASK AREA & WORK UNIT NUMBERS
11. CONTROLLING OFFICE NAME AND ADDRESS: Chemistry, Office of Naval Research, Arlington, VA 22217	12. REPORT DATE: May 29, 1987
	13. NUMBER OF PAGES: 19
14. MONITORING AGENCY NAME & ADDRESS(if different from Controlling Office)	15. SECURITY CLASS. (of this report): Unclassified
	15a. DECLASSIFICATION/DOWNGRADING SCHEDULE

16. DISTRIBUTION STATEMENT (of this Report)

Technical Report Distribution List, GEN/413-2.
For unlimited distribution and public release.

17. DISTRIBUTION STATEMENT (of the abstract entered in Block 20, if different from Report)

Abstracts Distribution List, 356A/413-2.
For unlimited distribution and public release.

18. SUPPLEMENTARY NOTES

Presented at National Meeting of American Institute of Chemical Engineers, August 24-27, 1986, Boston, MA

19. KEY WORDS (Continue on reverse side if necessary and identify by block number)

Poly (methyl methacrylate)
Dissolution
Transition layers
Microlithography

20. ABSTRACT (Continue on reverse side if necessary and identify by block number)

The technique of laser interferometry is now routinely used by the microelectronics industry for the measurement of the dissolution rates of thin polymer films. In addition to the rate of dissolution, laser interferometry can also provide quantitative information on the thickness of the transition layer between the dissolving glassy polymer and the liquid solvent. This paper describes how observed patterns of reflected light intensity may be analyzed to calculate the thickness of the transition layer for polymers that dissolve

DD FORM 1 JAN 73 1473 EDITION OF 1 NOV 65 IS OBSOLETE
S/N 0102-LF-014-6601

SECURITY CLASSIFICATION OF THIS PAGE (When Data Entered)

with little or no swelling. The technique required knowledge of the shape of the concentration profile in the transition layer. However, by assuming various simple model profiles one may obtain a reasonable estimate. Experimental measurements of PMMA films dissolving in methyl ethyl ketone indicate transition layers of thicknesses 0 to 0.1 μm for PMMA of molecular weights M_w = 37,000 to 1,400,000.

MEASURING AND MODELLING THE TRANSITION LAYER DURING THE DISSOLUTION OF GLASSY POLYMER FILMS

P.D. Krasicky, R.J. Groele, F. Rodriguez
School of Chemical Engineering, Olin Hall
Cornell University
Ithaca, NY 14853

INTRODUCTION

Over the past few years there has been a renewed interest in the study of polymer swelling and dissolution behavior. Most theoretical models have concentrated on diffusion and swelling,[1-7] but some work is also being done on dissolution.[8-10] The wide variety of observed phenomena is indicative of the complexity of the problem. Experimentally, many techniques and sample geometries have been used.[11] Optical microscopy[7,12,13] has proven useful for the study of swelling and dissolution behavior since it allows measurement of the rate of dissolution and observation of the concentration profile in the dissolving surface layer. However, microscopy works best when the dimensions being observed are 10 μm or greater. Rutherford Backscattering Spectroscopy[14] may be used to make measurements on much smaller dimensions, but since it cannot be done *in situ* and requires special sample preparation procedures, it is limited to the study of swelling only.

This paper was presented in part at the National Meeting of the Amer. Inst. of Chem. Engs., Boston, August 24-27, 1986.

Of particular interest to the microelectronics industry is the dissolution of a 1 μm thick polymer film on a silicon substrate. The technique of laser interferometry[8-11] is now routinely used for the screening of new polymer-solvent systems and for the optimization of processing conditions. Not so obvious in the use of laser interferometry is the quantitative information it can provide on the dissolving surface layer for polymers that dissolve with little or no swelling.

DISSOLUTION RATE MEASUREMENT USING LASER INTERFEROMETRY

Laser interferometry is popular as the method of dissolution rate measurement since the sample geometries and substrate materials of typical microlithographic processes can be used. The basic apparatus for laser interferometry is shown in figure 1. A silicon wafer that has been coated with a 0.5 to 1.5 μm thick film of polymer is suspended in a transparent cylindrical container filled with the developing solvent. The solvent container includes a magnetic stirrer and a heating/cooling coil connected to a temperature bath. The beam from an unpolarized He-Ne laser of wavelength 6328 Å is directed obliquely at the coated substrate with an incident angle of typically 10°. The reflected beam is collected by a silicon photocell and the recorded signal represents the reflected intensity as a function of time. A more complete description of the technique is given by Krasicky et. al..[11]

As the polymer film dissolves, the reflected intensity should oscillate due to thin film interference effects. The quantity of interest is the reflectance R which is defined as the ratio of the reflected light intensity to the incident light intensity. A sufficiently accurate expression for the reflectance R is

$$R = r_{s,p}^2 + 2r_{f,p}r_{s,f}(1-r_{s,f}^2)\cos\theta_f \qquad (1)$$

Here $r_{s,p}$ and $r_{f,p}$ are the Fresnel reflection coefficients for the polymer/substrate and solvent/polymer interfaces, respectively. The phase angle θ_f is the difference in phase between light rays reflected from the two interfaces. The phase angle is given by

$$\theta_f = \frac{4\pi d \sqrt{n_p^2 - n_f^2\sin^2\theta_f}}{\lambda} \qquad (2)$$

Where d is the thickness of the polymer film, λ is the free space wavelength of the light, θ_f is the incident angle of the light, and n_f and n_p are the refractive indices of the solvent and polymer. Figure 2 is a sketch of a typical observed reflected intensity pattern. As expected the reflected intensity oscillates sinusoidally until the film is completely dissolved, after which the reflectance from the bare substrate is constant. From a reflectance-time trace such as figure 2, measurement of

the reflectance ratio a/b and the period of oscillation T allows calculation of the dissolution rate of the polymer film and the polymer's refractive index. Values of the refractive indices of the substrate and solvent, the wavelength of light, and the incident angle must also be known.

The above analysis applies only if the solvent/polymer interface is perfectly sharp. For some polymer-solvent systems this interface is not perfectly sharp, but is expanded into a continuous transition layer of nonzero thickness. The appropriate expression for the reflectance is now

$$R = r_{1,2}^2 + 2f r_{1,2} r_{2,3} (1 - r_{1,2}^2) \cos\phi \qquad (3)$$

Here f is a positive factor less than unity multiplying the reflection coefficient $r_{1,2}$ and $\phi = \phi_2 + \phi_1$. Both f and the phase angle ϕ_1 depend on the thickness and shape of the concentration profile in the transition layer. The effect of the transition layer is to reduce the amplitude of the reflectance oscillations by the factor f while preserving the average value of the reflectance, and to shift the oscillations' phase by ϕ_1. The amplitude reduction factor f is measured as a gap or offset created between the maximum value of reflectance in the oscillations and the reflectance of the bare substrate after the film has completely dissolved (see figure 3).

$$f = \frac{a - b}{(a + s) - (b - s)} \qquad (4)$$

The phase angle $\emptyset_i$ is measured in terms of the time interval $t_\emptyset$ between the observed endpoint of dissolution and the next expected maximum relative to the period for a complete oscillation.

$$\emptyset_i = \left(\frac{t_\emptyset}{T}\right) 360° \tag{5}$$

Correction for Silicon Oxide Layer

A small correction needs to be made when a silicon wafer is used as the substrate material. A very thin layer of silicon oxide is always present and can account for an additional phase shift given approximately by

$$\emptyset_{ox} = \frac{4\pi d_{ox} n_{ox}}{\lambda} \tag{6}$$

where d_{ox} is the thickness of the silicon oxide layer, n_{ox} is its refractive index, and λ is the wavelength of light used. For the silicon substrates used in this work the thickness of the native oxide layer was measured by ellipsometry to be about 21 A. This can account for a phase shift of 3.5° which must be subtracted from the measured value of $\emptyset_i$ to get the phase shift due to the transition layer alone.

Surface Roughness

One might wonder whether an alternate explanation for the apparent reduction in the amplitude of the reflectance oscillations could be roughness on the dissolving polymer surface. Using simple scattering theory it can be shown that the presence of a rough surface at the polymer/solvent interface would result in a reduction of the amplitude of the reflectance oscillations, but the average value of the reflectance would also be reduced. If surface roughness were present one would calculate an erroneous polymer refractive index when applying the equations derived for the presence of a transition layer. For the polymers used in this study the refractive index was verified to be correct by other means. Thus it appears the formation of a transition layer is the correct explanation for the observed behavior.

QUANTITATIVE ANALYSIS OF THE TRANSITION LAYER

The magnitude of the observed amplitude reduction factor may be used as a gauge of the thickness of the transition layer between the solvent and the glassy polymer. A value of $f = 1$ would correspond to a perfectly sharp interface, i.e. a transition layer of zero thickness. Values of $f < 1$ correspond to thicker transition layers. A more quantitative analysis is also possible. In principle, one can calculate an absolute thickness

of the transition layer, provided the shape of the concentration profile is known. For simplicity, this profile may be expressed in terms of refractive index (as in figure 4). It can be shown that the variation in refractive index through the transition layer is to a good approximation proportional to the variation in concentration. It is assumed that the transition layer has a finite thickness δ and that the refractive index in the layer varies only in the direction perpendicular to the surface, for which the distance variable is z. The profile may be simplified further by scaling the variables of thickness and refractive index (see figure 5).

$$u = \frac{z}{\delta} \tag{7}$$

$$g(u) = \frac{n(u) - n_1}{n_2 - n_1} \tag{8}$$

The resulting expressions that quantify the transition layer can be derived from optical theory of inhomogeneous layers. The amplitude reduction factor f is equal to the magnitude of the complex quantity $F(\gamma)$ and the phase angle $\emptyset_1$ is the complex phase arg of $F(\gamma)$.

$$f = |F(\gamma)| \tag{9}$$

$$\emptyset_1 = \arg(F(\gamma)) \tag{10}$$

where

$$F(\gamma) = \int_{-\infty}^{\infty} e^{i\gamma u} \frac{-dg(u)}{du}\, du \tag{11}$$

$$\gamma = \delta/\ell \tag{12}$$

$$\ell = \frac{\lambda}{4\pi n_t \cos\theta_t} \tag{13}$$

$$n_t = \frac{n_1 + n_2}{2} \tag{14}$$

$$\cos\theta_t = \left[1 - \left(\frac{n_1 \sin\theta_1}{n_t}\right)^2\right]^{1/2} \tag{15}$$

Equation 11 for $F(\gamma)$ results when the reflection coefficient of the transition layer is calculated using the Rayleigh-Gans or Born approximation.[12,13] Physically, this amounts to treating the transition layer as a continuous weakly reflecting region in which the local differential reflection coefficient is $|\nabla n|/2n$,[14-17] where ∇n is the gradient of refractive index. Weakly reflecting means that the total change in refractive index is small compared with the average refractive index and that multiple reflections within the layer can be neglected. The overall reflection coefficient of the layer is found by integrating the differential reflection coefficient while incorporating the appropriate phase factor to account for propagation through

the layer. Scaling the parameters then gives $F(\gamma)$ in equation 11. Thus, one only needs to know something about the shape of the refractive index profile g(u) in order to calculate directly its thickness δ from the measured values of f and ϕ_c. If knowledge about the profile is incomplete, then a fitting procedure needs to be used to match the thickness δ to the measured f and ϕ_c.

EXPERIMENTAL RESULTS

Measurements were made on various molecular weights of PMMA dissolving in MEK at 20°C. As in figure 3, the presence of the transition layer is evident by the reduction in the amplitude of the reflectance oscillations. Also, the endpoint of dissolution often occurs significantly ahead of the next extrapolated maximum in intensity. Because the reflectance is not observed to deviate from its sinusoidal variation until the endpoint of dissolution, it is postulated that this point represents the "leading edge" of the transition layer. Once this point reaches the substrate surface the remaining transition layer dissolves away rapidly. Table 1 lists the measured values of f and ϕ_c for the various molecular weights of PMMA dissolving in MEK. These values are plotted in figure 6.

Thickness Calculations

In order to calculate directly the thickness of the transition layer it is necessary to know the shape of its refractive index profile. Unfortunately, the exact shape of this profile is not known for these types of polymer-solvent systems. However, it is still instructive to calculate the thickness based on some simple model profiles. The profile shapes (figure 7) of linear, cosine, step-linear, and step-exponential were chosen to approximate a realistic profile shape and still allow an analytical solution to the integral in Equation 11. The functional form of these profiles and their derivatives as they would appear in equation 11 are listed in Table 2.

The thickness of the transition layer can be calculated to match the measured values of f and $\emptyset_c$. The linear and cosine profiles contain only one adjustable parameter: the normalized transition layer thickness γ, so in general the observed values of f and $\emptyset_c$ cannot both be satisfied at the same time. The step-linear and step-exponential profiles contain two adjustable parameters: γ and the step fraction q. For the latter two profiles it is assumed that the observed endpoint of controlled uniform dissolution occurs when the step edge of the transition layer reaches the substrate surface. The occurrence of these step-like profiles has been observed on a much larger scale by Ueberreiter[7] in the dissolution of polystyrene.

In principle one could perform the above analysis for any profile shape, although it might require numerical integration

and tedious iteration to solve for the transition layer thickness. In practice it is convenient to use a graphical procedure. As an example, figure 8 is a chart of transition layer thickness as a function of phase shift for the step-linear profile, with γ and q as adjustable parameters. In this case one only needs to read off the unique values of normalized thickness γ and step fraction q for measured values of f and $\emptyset_{..}$

Table 3 lists the calculated thicknesses of the transition layer of PMMA for the four model profiles. Although not entirely obvious from the values given in Table 3 the actual physical thicknesses are very close for all four model profiles. This can be seen more clearly in figure 9 where the actual profiles have been plotted on the same scale for one molecular weight of PMMA. Despite deviations at the tail ends the profiles overlap remarkably well. Thus, even though the exact profile shape is not known, it is reasonable to conclude that the transition layer thickness calculated by any of the model profiles is not far from the actual thickness. The same kind of consistency in overall thickness has been obtained elsewhere by fitting a family of one-parameter refractive index profiles to photometry data from the reflection of light from an interface separating the liquid and vapor phases of a fluid near its critical point.[14]

CONCLUSIONS

The technique just described is useful for approximating the thickness of the transition layer for polymers that dissolve with little or no swelling. Because the calculated thickness does not depend strongly on the assumed concentration profile shape it is reasonable that a calculated thickness will closely approximate the actual thickness. However, for the same reason experimental measurements are not likely to distinguish among various theoretical models based on profile shape alone. Application of this technique to polymer-solvent systems that exhibit both swelling and dissolution is not as straightforward since these systems are generally characterized by a non-uniform dissolution rate and damped reflectance oscillations, i.e. T and f are not constant. However, at least some qualitative information about the profile may be obtainable in such cases.

The reflectance of the dissolving film is not observed to deviate from its sinusoidal shape until the leading edge of the transition layer reaches the substrate surface. At that time the remaining transition layer dissolves away rapidly. It appears that the rate of the dissolution process is governed primarily by what is happening near the leading edge -- the interface with the solid polymer -- rather than by what is happening elsewhere in the transition layer. Although it does not provide direct detailed information about the shape of the concentration profile in the transition layer, this technique may be helpful in the

development of theoretical models for the dissolution of polymers by revealing the length scales over which the dissolution process takes place.

ACKNOWLEDGEMENTS

This work was supported in part by the Office of Naval Research. The cooperation of the National Research and Resource Facility for Submicron Structures at Cornell (with sponsorship by NSF) also is acknowledged.

REFERENCES

1. A.H. Windle, in "Polymer Permeability," ed. J. Comyn, Elsevier Applied Science Publishers, London (1985).
2. J.S. Vrentas, J.L. Duda, and A.-C. Hou, Journal of App. Polymer Science, 29, 399 (1984).
3. C. Gostoli, and G.C. Sarti, Polym. Eng. Sci., 22, 1018 (1982).
4. R.C. Lasky, PhD Thesis, Cornell University (1986).
5. A.C. Ouano, in "Polymers in Electronics," ACS Symposium Series, 242, ed. T. Davidson, ACS, Washington D.C. (1984).
6. D.S. Soong, SPIE Proceedings, 539, ed. L.F. Thompson, (March, 1985).
7. E.E Parsonage, N.A. Peppas, and P.I. Lee, paper to be published, Journal of Vacuum Science and Tech., B.
8. F. Rodriguez, P.D. Krasicky, and R.J. Groele, Solid State Technology, 28, 125 (May, 1985).

9. K. Ueberreiter, in "Diffusion in Polymers," ed. J. Crank and G.S. Park, Academic Press, New York (1968).

10. A.C. Ouano, Y.O Tu, and J.A. Carothers, in "Structure-Solubility Relationships in Polymers," ed. F.W. Harris and R.B. Seymour, Academic Press, New York (1977).

11. P.D. Krasicky, R.J. Groele, and F. Rodriguez, paper to be published, Chem. Eng. Comm..

12. Lord Rayleigh, Proc. Roy. Soc. A 86, 207 (1912).

13. R. Gans, Ann. Physik 47, 707 (1915).

14. W. Geffcken, Ann. d. Phys. (5) 40, 385 (1941).

15. R. Jacobsson, Progress in Optics 5, 247 (1965).

16. J.S. Huang and W.W. Webb, J. Chem. Phys. 50, 3677 (1969).

TABLE 1: Amplitude reduction factor f, and phase shift angle ϕ_t, due to the transition layer for various molecular weights of PMMA dissolving in MEK at 20°C.

Molecular Weight M_w	Molecular Weight M_w	f	ϕ_t (degrees)
27×10^3	37×10^3	1.0	4
29	52	1.0	4
34	61	1.0	4
35	63	0.97	9
67	134	0.93	8
97	170	0.90	12
100	150	0.89	10
160	320	0.89	25
180	270	0.88	15
220	500	0.85	24
220	500	0.87	30
360	950	0.79	30
360	950	0.80	33
1000	1400	0.71	35

TABLE 2

MODEL TRANSITION LAYER CONCENTRATION PROFILES

PROFILE SHAPE	g(u)	dg(u)/du*
1. LINEAR	$1 - u$	-1
2. COSINE	$0.5(1 + \cos\pi u)$	$-0.5\pi\sin\pi u$
3. STEP-LINEAR	$q(1 - u)$	$-q - (1 - q)\delta(u)$
4. STEP-EXPONENTIAL	$qe^{-\ln(1/q)u}$	$-qe^{-\ln(1/q)u} - (1 - q)\delta(u)$

* Note that here $\delta(u)$ represents the Dirac delta function and is necessary to account for reflection at the step portion of the profile in equation 11. It should not be confused with the transition layer thickness δ elsewhere in the text.

TABLE 3: Calculated transition layer thickness δ, and step fraction q, for PMMA using various model profile shapes. Units of δ are micrometers.

Molecular Weight		Linear	Cosine	Step-linear		Step-exp.	
M_n	M_w	δ	δ	δ	q	δ	q
27 x 10^3	37 x 10^3	0	0	0	0	0	1
29	52	0	0	0	0	0	1
34	61	0	0	0	0	0	1
35	63	0.031	0.041	0.027	0.40	0.013	0.40
67	134	0.047	0.063	0.053	0.19	0.022	0.28
97	170	0.057	0.075	0.063	0.27	0.023	0.41
100	150	0.060	0.079	0.074	0.22	0.029	0.32
160	320	0.060	0.079	0.053	0.63	0.019	0.80
180	270	0.062	0.083	0.065	0.34	0.024	0.50
220	500	0.070	0.093	0.063	0.52	0.023	0.76
220	500	0.065	0.086	0.057	0.68	0.021	1.0
360	950	0.084	0.11	0.076	0.56	0.030	0.81
360	950	0.081	0.11	0.071	0.62	0.028	0.90
1000	1400	0.10	0.13	0.079	0.54	0.038	0.82

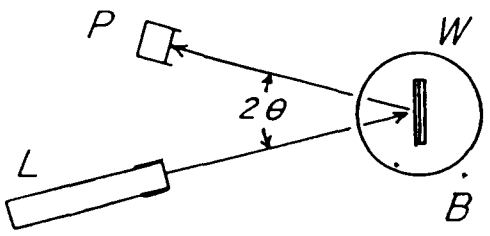

1. Interferometer for monitoring polymer dissolution. Beam from laser, L, is reflected at angle θ from coated wafer, W, immersed in solvent bath, B. Reflected light is measured with photocell, P.

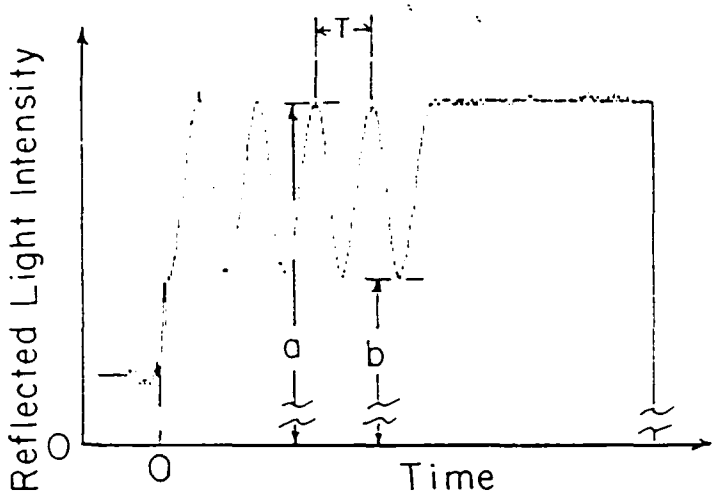

2. Typical reflected light intensity trace from polymer film with a negligible transition layer. This example used a personal computer interfaced with the photocell to reproduce the signal. The period T and amplitudes a and b are used to calculate the dissolution rate.

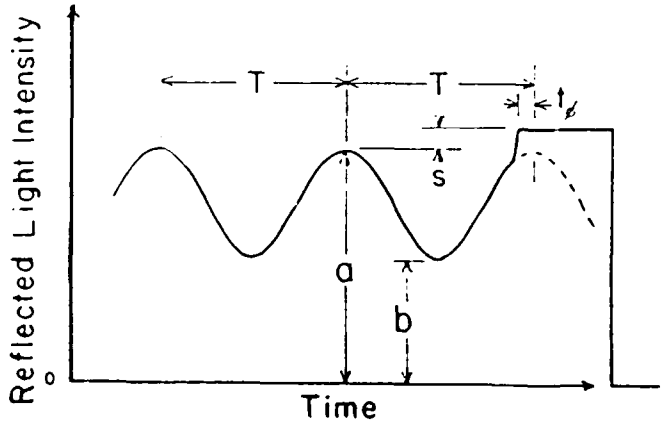

3. Trace of reflected light intensity when transition layer is present. The added features (beyond Fig. 2) are the offset, s, and the phase difference, t_ϕ.

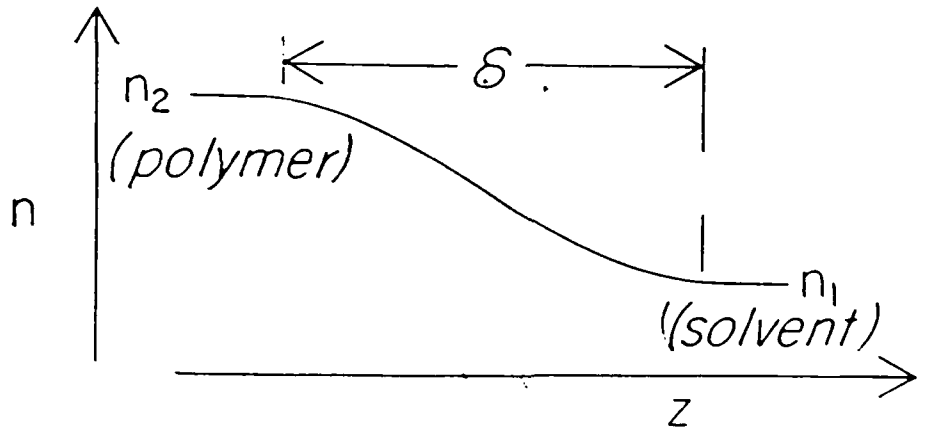

4. Refractive index n. profile in the transition layer of thickness δ where z is distance

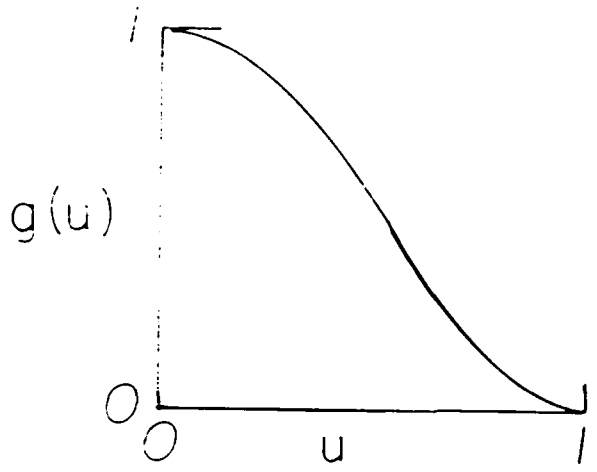

5. Scaled refractive index profile where u and g(u) are given by equations 7 and 8.

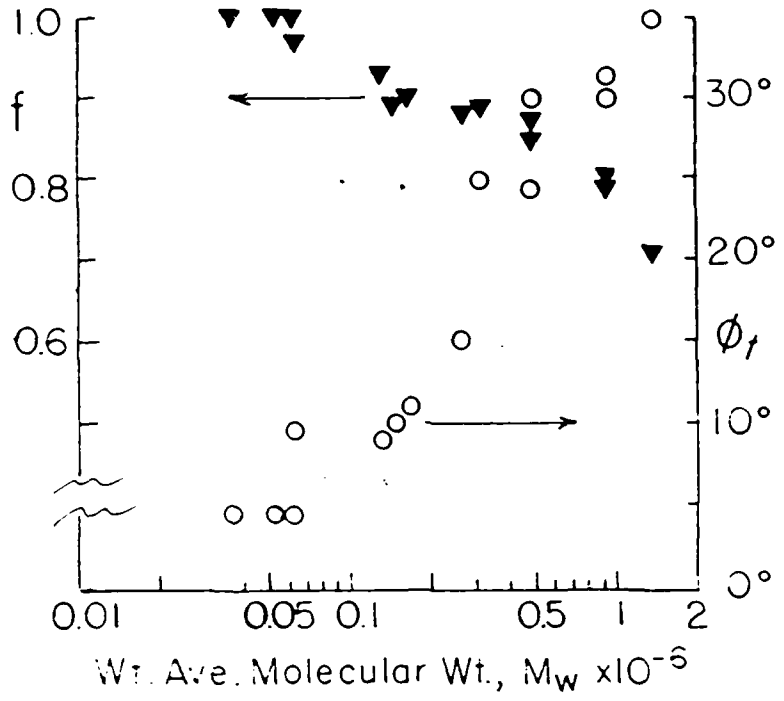

6. Experimental results for PMMA dissolving in MEK at 20°C where f is the Amplitude reduction factor and θ_t is the Phase shift angle (see equations 4 and 5).

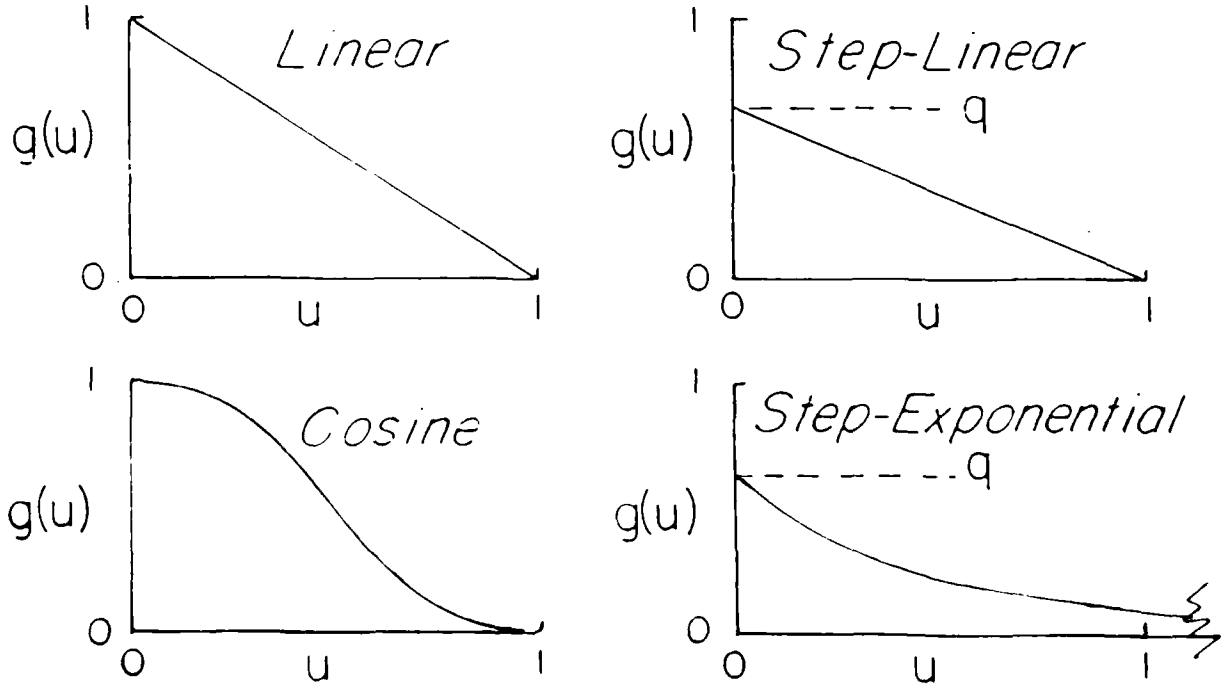

7. Profiles for the four models of Table 2.

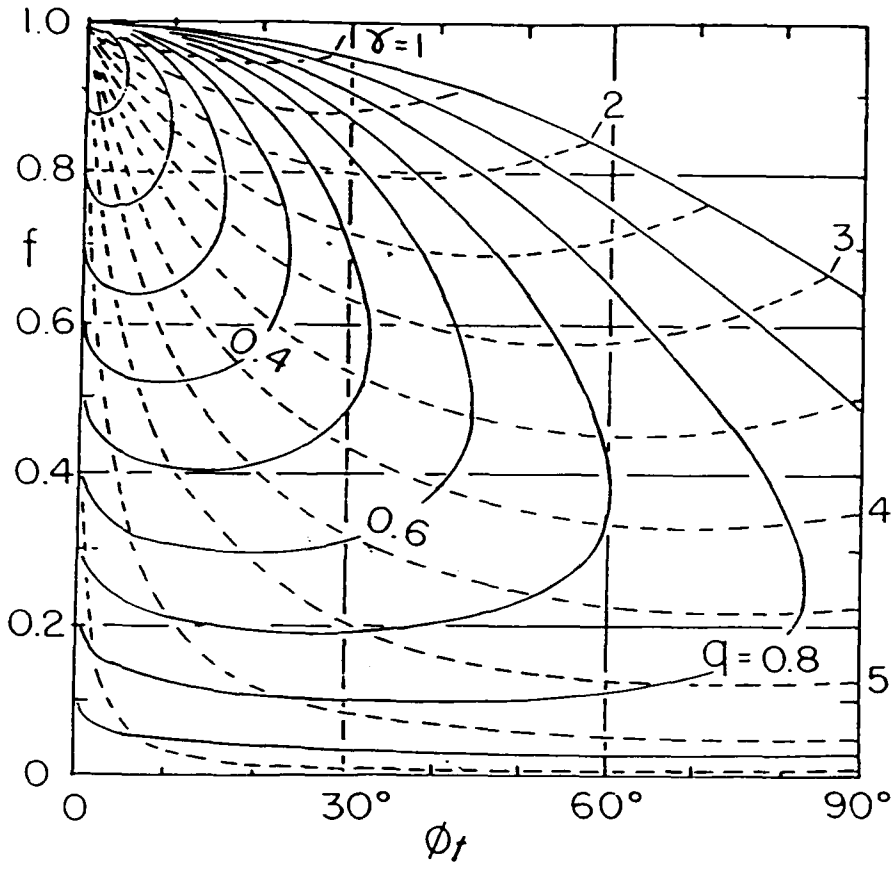

8 Chart of reduced transition layer thickness, γ, as a function of the measured Amplitude reduction factor, f, and the Phase shift angle, θ_t. The parameter q takes into account the step change in concentration at the polymer-transition interface.

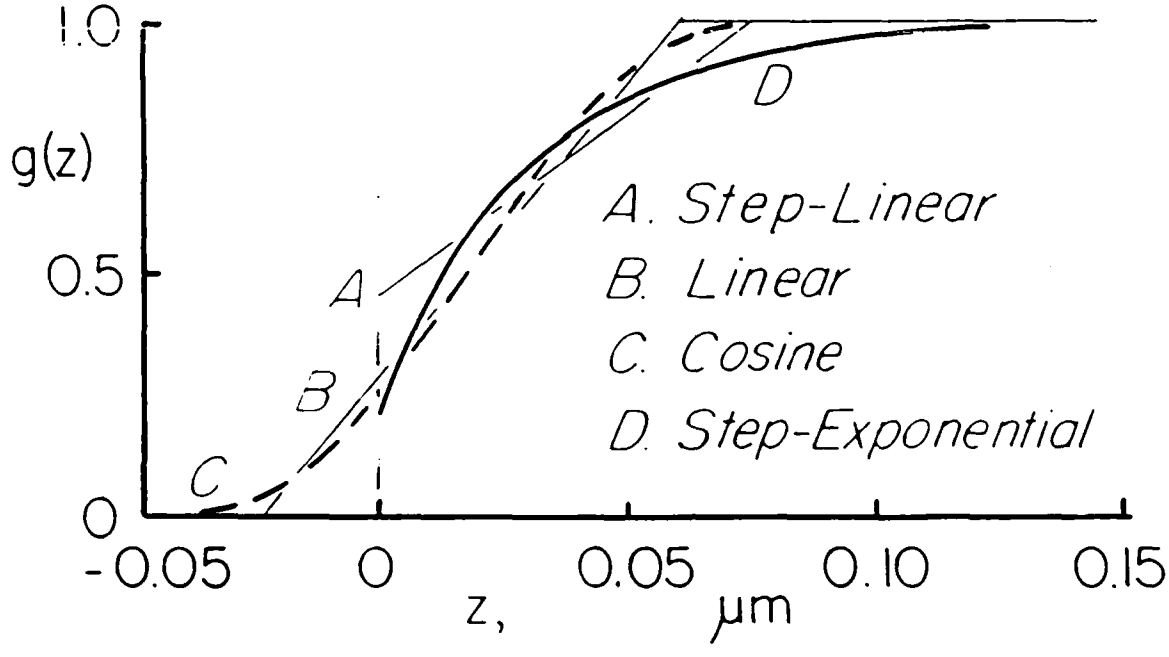

9. The experimentally fitted model profiles are seen to be almost indistinguishable from each other for all four models. The data used here are for PMMA of M_w = 950,000 in MEK at 20°C.

OL/413/83/01
GEN/413-2

TECHNICAL REPORT DISTRIBUTION LIST, GEN

	No. Copies
Office of Naval Research Attn: Code 413 800 N. Quincy Street Arlington, Virginia 22217	2
Dr. Bernard Douda Naval Weapons Support Center Code 5042 Crane, Indiana 47522	1
Commander, Naval Air Systems Command Attn: Code 310C (H. Rosenwasser) Washington, D.C. 20360	1
Naval Civil Engineering Laboratory Attn: Dr. R. W. Drisko Port Hueneme, California 93401	1
Defense Technical Information Center Building 5, Cameron Station Alexandria, Virginia 22314	12
DTNSRDC Attn: Dr. G. Bosmajian Applied Chemistry Division Annapolis, Maryland 21401	1
Dr. William Tolles Superintendent Chemistry Division, Code 6100 Naval Research Laboratory Washington, D.C. 20375	1
Dr. David Young Code 334 NORDA NSTL, Mississippi 39529	1
Naval Weapons Center Attn: Dr. Ron Atkins Chemistry Division China Lake, California 93555	1
Scientific Advisor Commandant of the Marine Corps Code RD-1 Washington, D.C. 20380	1
U.S. Army Research Office Attn: CRD-AA-IP P.O. Box 12211 Research Triangle Park, NC 27709	1
Mr. John Boyle Materials Branch Naval Ship Engineering Center Philadelphia, Pennsylvania 19112	1
Naval Ocean Systems Center Attn: Dr. S. Yamamoto Marine Sciences Division San Diego, California 91232	1

ABSTRACTS DISTRIBUTION LIST, 356A

Naval Surface Weapons Center
Attn: Dr. J. M. Augl, Dr. B. Hartman
White Oak
Silver Spring, Maryland 20910

Professor Hatsuo Ishida
Department of Macromolecular Science
Case Western Reserve University
Cleveland, Ohio 44106

Dr. Robert E. Cohen
Chemical Engineering Department
Massachusetts Institute of Technology
Cambridge, Massachusetts 02139

Dr. R. S. Porter
Department of Polymer Science
and Engineering
University of Massachusetts
Amherst, Massachusetts 01002

Professor A. Heeger
Department of Chemistry
University of California
Santa Barbara, California 93106

Dr. T. J. Reinhart, Jr., Chief
Nonmetallic Materials Division
Department of the Air Force
Air Force Materials Laboratory (AFSC)
Wright-Patterson AFB, Ohio 45433

Professor J. Lando
Department of Macromolecular Science
Case Western Reserve University
Cleveland, Ohio 44106

Professor C. Chung
Department of Materials Engineering
Rensselaer Polytechnic Institute
Troy, New York 12181

Professor J. T. Koberstein
Department of Chemical Engineering
Princeton University
Princeton, New Jersey 08544

Professor J. H. Magill
Department of Metallurgical
and Materials Engineering
University of Pittsburgh
Pittsburgh, Pennsylvania 15261

Professor J. K. Gillham
Department of Chemistry
Princeton University
Princeton, New Jersey 08540

Professor R. S. Roe
Department of Materials Science
and Metallurgical Engineering
University of Cincinnati
Cincinnati, Ohio 45221

Professor L. H. Sperling
Department of Chemical Engineering
Lehigh University
Bethlehem, Pennsylvania 18015

Professor Brian Newman
Department of Mechanics and
Materials Science
Rutgers University
Piscataway, New Jersey 08854

Dr. C. E. Hoyle
Department of Polymer Science
University of Southern Mississippi
Hattiesburg, Mississippi 39406

Dr. Stuart L. Cooper
Department of Chemical Engineering
University of Wisconsin
Madison, Wisconsin 53706

Professor D. Grubb
Department of Materials Science
and Engineering
Cornell University
Ithaca, New York 14853

Dr. D. B. Cotts
SRI International
333 Ravenswood Avenue
Menlo Park, California 94205

PLASTEC
DRSMC-SCM-O(D), Bldg 351 N
Armament Research & Development
Center
Dover, New Jersey 07801

Professor C. H. Wang
Department of Chemistry
University of Utah
Salt Lake City, Utah 84112

END

7-87

DTIC